

*Received July 9, 2015; reviewed; accepted November 25, 2015*

## ADSORPTION MECHANISM OF SODIUM OLEATE ON TITANIUM DIOXIDE COATED SENSOR SURFACE USING QUARTZ CRYSTAL MICROBALANCE WITH DISSIPATION

Guixia FAN<sup>\*</sup>, Jiongtian LIU<sup>\*,\*\*</sup>, Yijun CAO<sup>\*\*</sup>, Li FENG<sup>\*\*</sup>, Hongxiang XU<sup>\*\*\*</sup>

<sup>\*</sup> School of Chemical Engineering and Energy, Zhengzhou University, Zhengzhou 450001, China

<sup>\*\*</sup> National Engineering Research Center of Coal Preparation and Purification, Xuzhou 221116, Jiangsu, China

<sup>\*\*\*</sup> School of Chemical and Environmental Engineering, University of Mining and Technology (Beijing), Beijing, China, 100083, fangx1029@163.com (Fan Guixia), yijuncao@126.com (Cao Yijun)

**Abstract:** Quartz Crystal Microbalance with Dissipation (QCM-D) was firstly applied to investigate the adsorption mechanism of sodium oleate on TiO<sub>2</sub> coated sensor surface. The effects of pH value, sodium oleate concentration, and temperature on TiO<sub>2</sub> coated sensor surface were evaluated systematically using the QCM-D technique. Zeta potential, surface tension, adsorption isotherms, and adsorption thermodynamics were employed to characterize the adsorption process. The results showed the advantages of QCM-D on the investigation of the adsorption process. Additionally, the electrostatic equilibrium adsorption data was well matched to the Langmuir isotherm. Based on the thermodynamic analysis, adsorption was a spontaneous and endothermic physisorption process.

**Keywords:** QCM-D, TiO<sub>2</sub> coated sensor surface, sodium oleate, adsorption mechanism

### Introduction

Titanium is an important raw material for space industry, nautical engineering, and medicine (Li et al., 2006; Omidvar et al., 2012; Parker and Stec, 2012). Flotation, as an efficient physicochemical technique, is widely used in rutile and ilmenite upgrading (Hacifazlioglu and Sutcu, 2007; Santana et al., 2012). In flotation systems, adsorption mechanism between titanium minerals and collectors is the key for flotation (Fan and Rowson, 2000; 2002). Evaluation of adsorption behavior is essential and helpful for developing efficient collectors, thereby to understand the adsorption mechanism well (Kou et al., 2010). Generally, sodium oleate is used as a collector for flotation of ilmenite (Fan et al., 2014), talc (Yakovleva and Chyong, 2013), fluorite, and hematite (Chanturia and Kondrat'ev, 2014), and so on. However, quantitative analysis on the

adsorption of sodium oleate is a tough work because of low adsorption mass and difficulties in detection (Alagha et al., 2013; Irwin et al., 2005).

Quartz Crystal Microbalance with Dissipation (QCM-D) is a technique to detect minute mass changes (nanogram range) on the surface of an electro-acoustical sensor device, mainly in a form of a thin slice of quartz crystal, by detecting changes of its resonance behavior (Buttry and Ward, 1992; Vittorias et al., 2010). Recently, *in situ* QCM-D is known as a reliable method to monitor the adsorption kinetics of nanoparticles (Strydom et al., 2014), DNA (Song et al., 2014), artificial skeleton (Lilja et al., 2013), proteins (Ebara and Okahata, 1994), and polymers (Marx, 2003). QCM-D is also a powerful tool for investigating the interactions between solids and surfactants in solution (Bereket and Yurt, 2002; Simbeck et al., 2011).

In this work, the adsorption process of sodium oleate on TiO<sub>2</sub> coated sensor surface was studied using QCM-D in order to reveal the adsorption mechanism of sodium oleate on titanium mineral. The effects of pH value, sodium oleate concentration, and temperature of sodium oleate solution on TiO<sub>2</sub> coated sensor surface were evaluated. Finally, the adsorption isotherms and adsorption thermodynamics were analyzed to explain the adsorption process.

## Experimental

### Material and reagents

The quartz crystal sensors with TiO<sub>2</sub> coatings crystals were purchased from Q-Sense (BiolinScientific, Q-Sense, Sweden). Analytical grade (99.70%) sodium oleate (C<sub>17</sub>H<sub>33</sub>COONa), sodium acetate, acetic acid, and sodium dodecyl sulfate (SDS) were purchased from Sinopharm Group of China. Generally, flotation of titanium minerals is performed under acidic conditions (Fan et al., 2009). Therefore, electrolyte solution with pH values of 3.5, 5.0, 6.0, and 7.5 were prepared using sodium acetate (0.2 mol/dm<sup>3</sup>) and acetic acid (0.2 mol/dm<sup>3</sup>). Then, sodium oleate was dissolved in the electrolyte solution at concentrations of 20, 50, 100, 150, and 200 mg/dm<sup>3</sup>. The ultrapure water (resistivity is 18.25 MΩ·cm) was prepared using water purification system (Millipore, USA).

The 97% pure rutile was obtained from natural rutile sample after a series of purification. For the zeta potential measurement the rutile sample was crushed to -2 μm.

### QCM-D measurements

The QCM-D measurements were performed with a Q-Sense E4 unit, which simultaneously monitors the changes in frequency ( $\Delta f$ ) and energy dissipation ( $\Delta D$ ) of a quartz crystal sensor. The QCM-D technique were reported in literature (Sakai et al., 2006; Yang et al., 2007). For rigid and thin adsorption layers ( $\Delta D < 10^{-6}$ ),  $\Delta f$  is direct proportion to mass through the Sauerbrey (1959) relationship:

$$\Delta m = -\frac{C \cdot \Delta f}{n} \quad (1)$$

where  $C$  is the mass sensitivity constant with its value of  $17.7 \text{ ng} \cdot \text{cm}^{-2} \cdot \text{Hz}^{-1}$  (Sauerbrey, 1959; Lilja et al., 2013). The  $\Delta f$  is the shift in frequency. The  $n$  parameter is the overtone ( $n = 1, 3, 5, 7, 9, 11$  or  $13$ ) of the resonance frequency of the applied voltage across the electrodes. Normalized frequency shifts at the third overtone are used to interpret the adsorption result (Deng et al., 2014). However, the Sauerbrey equation is limited for the case of thick and/or viscoelastic films. Fortunately, a new model for QCM-D operation in liquid was proposed by Kanazawa and Gordon (Kanazawa and Gordon, 1985; Schumacher et al., 1985). The resonant  $\Delta f$  can be described as:

$$\Delta f = -\frac{f_0^{3/2}}{\sqrt{\pi \rho_q \mu_q}} \sqrt{\eta_l \rho_l} \quad (2)$$

where  $f_0$ ,  $\mu_q$  and  $\rho_q$  are the characteristic resonant frequency, shear modulus and density of the quartz crystal, respectively, while the  $\rho_l$  and  $\eta_l$  are the density and viscosity of the liquid.

The  $\Delta D$  is proportional to the power dissipation in the oscillatory system, which provides information on rigidity of the attached materials. The dissipation is defined as:

$$\Delta D = \frac{E_{lost}}{2\pi E_{stored}} \quad (3)$$

where  $E_{lost}$  is the energy lost during one oscillation cycle,  $E_{stored}$  is the total energy stored in the oscillator. Because the  $\Delta D$  is a ratio of energies, it is dimensionless, and is reported as  $10^{-6}$  dissipation units.

However, while adsorption causes a great shift in the  $\Delta D$  value ( $\Delta D > 10^{-6}$ ), as a result of the adsorption of a viscous and soft layer. The adsorbed mass was fitted based on the Voigt model with the Q-tools software from Q-Sense AB. According to the Voigt model for viscous adsorption layer,  $\Delta f$  and  $\Delta D$  depend on the density ( $\rho$ ), thickness ( $h$ ), elastic shear modulus ( $\mu$ ), and shear viscosity ( $\eta$ ) of the adsorption layer (Alagha et al., 2013).

The  $-\Delta D/\Delta f$  means the energy dissipation per unit resonant frequency, which is used for characterizing the adsorption strength (Nezu et al., 2008). A more rigid and compact adsorption layer attached to the quartz crystal gives a low  $-\Delta D/\Delta f$  value. In contrast, a soft and dissipated layer gives a higher  $-\Delta D/\Delta f$  value.

For each experiment, the  $\text{TiO}_2$  coated quartz crystals were cleaned in a UV-Ozone chamber for 10 min prior to use. The  $\text{TiO}_2$  sensors were then mounted in four separate QCM-D flow chambers. A stable baseline was achieved firstly using sodium acetate and acetic acid electrolyte solution at the pH of interest, and then followed by introducing sodium oleate solutions. The baseline solutions were pumped into the flow

chamber when the frequency shift reaches plateau to remove loosely adsorbed or deposited layers. The  $\text{TiO}_2$  sensors were first ultra sonicated for 20 min in 5% SDS solution. Then, they were rinsed with the ultrapure water, and cleaned using UV Ozone for 20 min. Finally, they were rinsed thoroughly with the water again, and dried with nitrogen.

### Zeta potential measurements

The zeta potential values of rutile particles at different pH values were obtained from electrophoretic mobility measurements using a Brookhaven ZetaPALS (USA). The experiments were repeated at least three times (prepared on different days). In the tests, the concentrate of rutile suspensions was  $100 \text{ mg/dm}^3$  in the pH range of 3.0 ~ 8.0, and conditioned for 24 h to reach the adsorption equilibrium. The experiments were carried out at 298 K.

### Surface tension measurements

The surface tension measurements for the sodium oleate solution were performed using a Kruss K100 (Germany). The tensile force acting on the plate when in contact with the solution interface is measured and used to calculate the surface tension (Ryu and Free, 2003).

## Results and discussion

### Effect of pH value of sodium oleate solution on $\text{TiO}_2$ coated sensor surface

The pH value of sodium oleate solution has significant impact on the adsorption of  $\text{TiO}_2$  coated sensor surface (Fig. 1).

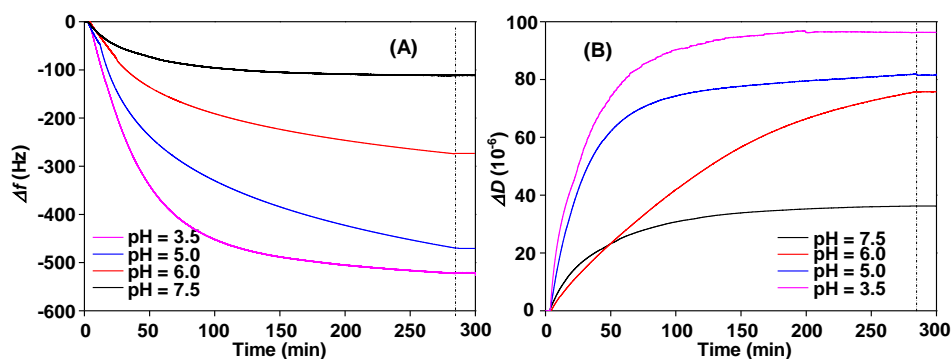


Fig. 1. QCM-D  $\Delta f$  and  $\Delta D$  response of third overtone as a function of time of the adsorption of sodium oleate on  $\text{TiO}_2$  surface with different pH values (sodium oleate concentration =  $100 \text{ mg/dm}^3$ ,  $T = 298 \text{ K}$ )

For a certain pH value, a rapid decrease in  $\Delta f$  (Fig. 1A) accompanied with a rapid increase in  $\Delta D$  (Fig. 1B). The changes of  $\Delta f$  and  $\Delta D$  at different pH values follow this

order: pH 3.5 > pH 5.0 > pH 6.0 > pH 7.5 from 0 to 285 min. The  $\Delta D$  is related to the thickness and viscoelasticity of the adsorbed layer. A lower pH value causes a much larger  $\Delta D$ , owing to the higher energy dissipation. In addition, a positive  $\Delta D$  indicates a soft structure. From 285 to 300 min,  $\Delta f$  and  $\Delta D$  were stable while the baseline solution was pumped into the system.

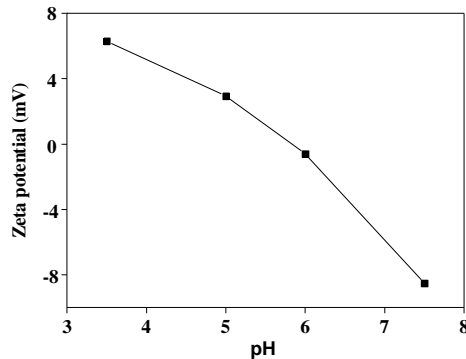


Fig. 2. Effect of pH values on zeta potentials of rutile

Figure 2 shows that the relationship between the zeta potentials of rutile and pH values. The isoelectric point of  $\text{TiO}_2$  is located at pH 5.9, implying  $\text{TiO}_2$  coated sensor surface is positively charged with pH < 5.9 and negatively charged with pH > 5.9. The carboxylate radical is the active site of sodium oleate, *i.e.* sodium oleate is negatively charged. Therefore, an electrostatic interaction occurred between  $\text{TiO}_2$  and sodium oleate solution. A remarkable adsorption on  $\text{TiO}_2$  coated sensor surface at pH 3.5 due to the electrostatic attraction between the positively charged  $\text{TiO}_2$  coated sensor surface and the negatively charged sodium oleate (Nezu et al, 2008). The adsorption behaviors at pH 6.0 and 7.5 are weaker than those at pH 3.5 and 5.0 because of the electrostatic repulsion between the negatively charged  $\text{TiO}_2$  coated sensor surface and the negatively charged sodium oleate.

### Effect of concentrate of sodium oleate solution on $\text{TiO}_2$ coated sensor surface

As Fig. 3 displays, the  $\Delta f$  changes sharply while sodium oleate was injected into the measurement chamber. Decreases of the  $\Delta f$  was observed with the increases of sodium oleate concentrate at one time. However, the  $\Delta f$  tends towards stable while sodium oleate concentrate is  $200 \text{ mg/dm}^3$ . As demonstrated in Fig. 3B, the adsorbed sodium oleate layer on  $\text{TiO}_2$  coated sensor surface is more rigid as the sodium oleate concentrate increases. In other words, the sodium oleate adsorption on  $\text{TiO}_2$  coated sensor surface is stronger as the concentrate strength increases.

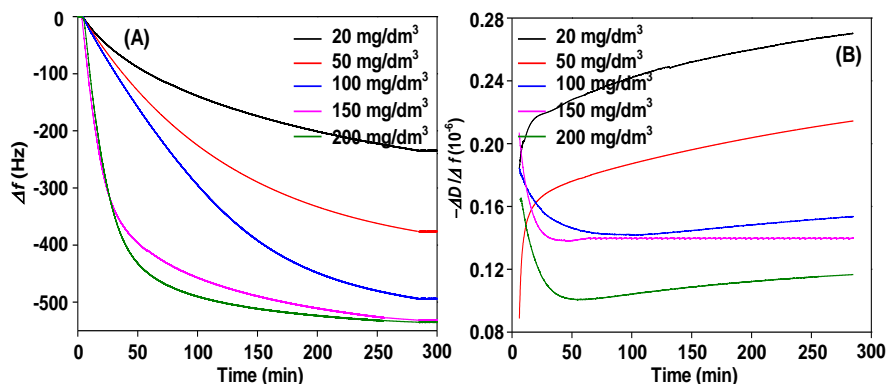


Fig. 3. QCM-D  $\Delta f$  and  $-\Delta D/\Delta f$  response of third overtone as a function of time of the adsorption of sodium oleate on  $\text{TiO}_2$  surface in different concentration (pH = 5.0,  $T = 298$  K)

### Adsorption isotherms

Adsorption isotherms are of importance because they can reflect the surface characteristics of the adsorbent at micro level, as well as the adsorption characteristics of adsorption mass and absorption state. As shown in Fig. 3A, the adsorption equilibrium is nearly reached at 285 min. As Fig. 4 describes, the adsorbed mass with different sodium oleate concentration was performed using the Voight model. Adsorption equilibrium data (at 285 min) was fitted by Langmuir and Freundlich equations as follows:

$$\frac{C_e}{\Gamma_e} = \frac{C_e}{\Gamma_m} + \frac{1}{K_L \Gamma_m} \quad (4)$$

$$\ln \Gamma_e = \ln K_f + \frac{1}{n} \ln C_e \quad (5)$$

where  $\Gamma_e$  ( $\text{mg}/\text{m}^2$ ) and  $\Gamma_m$  ( $\text{mg}/\text{m}^2$ ) represent the equilibrium absorption mass and the saturation absorption mass, respectively;  $K_L$  ( $\text{dm}^3/\text{mg}$ ) is the Langmuir constants involved in adsorption rate;  $C_e$  ( $\text{mg}/\text{dm}^3$ ) is the equilibrium concentration;  $K_f$  ( $\text{mg}/\text{m}^2$ ) and  $n$  are Freundlich constants.

The Langmuir and Freundlich isotherms are shown in Fig. 5.  $K_L$ ,  $\Gamma_m$ ,  $K_f$ , and  $n$  were determined from the two isotherms, and the values were presented in Table 1. The  $R^2$  (0.9977) of Langmuir model is very close to 1, and larger than that of Freundlich model (0.9766), indicating a good agreement with Langmuir model. The saturation adsorption mass calculated from the Langmuir isotherm is  $111.47 \text{ mg}/\text{m}^2$ , which approaches the experimental data ( $109.90 \text{ mg}/\text{m}^2$  from Fig. 4). Therefore, the adsorption layer is considered as physical absorption of monolayer adsorption which is consistent with electrostatic adsorption (Padilla-Ortega et al., 2014; Cui et al., 2014).

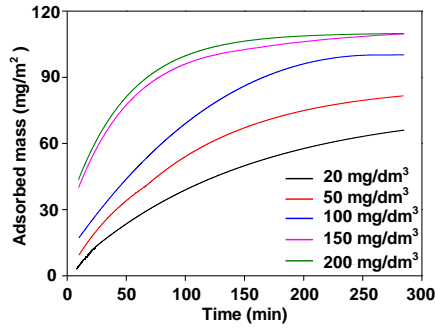


Fig. 4. The fitting adsorbed mass change with time with different sodium oleate concentration (pH = 5.0, T = 298 K)

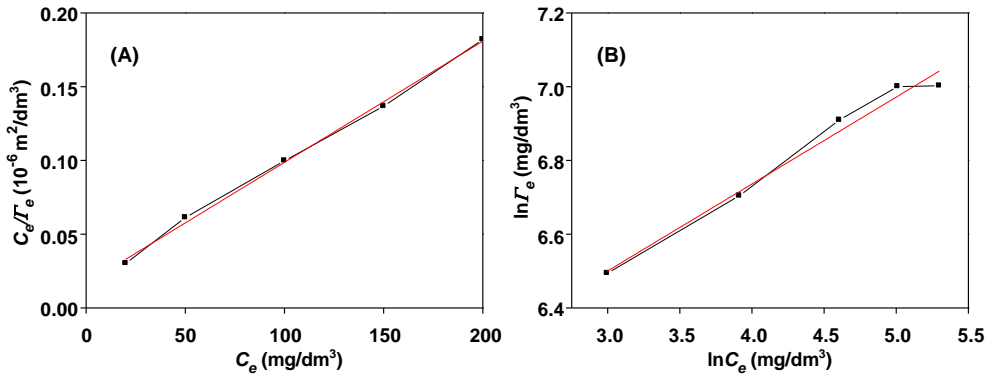


Fig. 5. Langmuir (A) and Freundlich (B) isotherm for the adsorption of sodium oleate on TiO<sub>2</sub> surface at 298 K

Table 1. Isotherm parameters for sodium oleate adsorption on TiO<sub>2</sub> at 298 K

Isotherms	Parameters	R <sup>2</sup>
Langmuir	$\Gamma_m = 111.47 \text{ (mg/m}^2\text{)}$	0.9977
	$K_L = 0.5407 \text{ (dm}^3\text{/mg)}$	
Freundlich	$K_f = 328.27 \text{ (mg/m}^2\text{)}$ $n = 4.2445$	0.9766

### Critical micelle concentration (CMC) of sodium oleate solution

Surfactant adsorption is affected by hydrocarbon chain length and solution ionic strength (Kim et al., 1998; Somasundaran and Huang, 2000; Fleming et al., 2001). As the surfactant concentration increases, the monomers tend to aggregate, resulting in lower surface tension. Adsorption of surfactant molecules at air-liquid interface is related to the lowering of surface tension according to the Gibbs adsorption equation:

$$\Gamma_i = -\frac{C}{RT} \left( \frac{\partial \gamma}{\partial C} \right)_{T,P} \quad (6)$$

where  $\gamma$ ,  $\Gamma_i$ ,  $R$ ,  $T$ , and  $C$  are surface tension (mN/m), adsorbed mass ( $\text{mg}/\text{m}^2$ ), molar gas constant ( $8.314 \text{ J}/(\text{mol}\cdot\text{K})$ ), absolute temperature (K), and surfactant concentration ( $\text{mg}/\text{dm}^3$ ), respectively.

As stated, the Langmuir adsorption layer is considered as monolayer adsorption. Thus, monolayer-level adsorbed mass increases as surface tension decreases. As monolayer coverage at the air-liquid interface is completed, the surface tension reaches a minimum plateau value. This point is considered as CMC. As demonstrated in Fig. 6, the surface tension decreases with the sodium oleate concentrate increases. The CMC of sodium oleate surfactant is  $173.42 \text{ mg}/\text{dm}^3$ . Therefore, the adsorbed mass little or nothing changes while the sodium oleate concentrate is greater than  $173.42 \text{ mg}/\text{dm}^3$ . This could provide a good explanation for Figs. 3A and 4, both of  $\Delta f$  and adsorbed mass only have a tiny change, when sodium oleate concentrate are  $150 \text{ mg}/\text{dm}^3$  and  $200 \text{ mg}/\text{dm}^3$ .

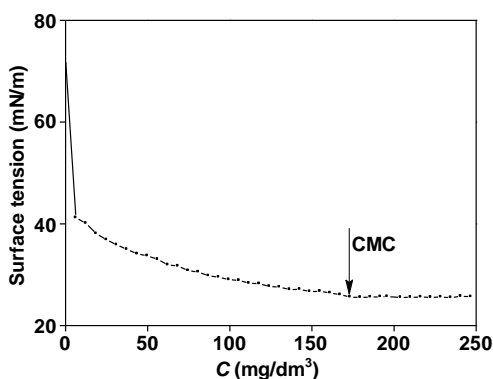


Fig. 6. Surface tension of sodium oleate solution

### Adsorption thermodynamics

Adsorption thermodynamics shows the energy effects in the process of adsorption, reflecting whether an adsorption process takes place under certain conditions (Guerra et al., 2014; Fu et al., 2015). The adsorption thermodynamics of sodium oleate ( $100 \text{ mg}/\text{dm}^3$ ) on  $\text{TiO}_2$  coated sensor surface were carried out at different temperatures (298, 303, 308, 313, and 318 K) at  $\text{pH} = 5.0$ . The data was fitted by the Voigt model and depicted in Fig. 7. The adsorbed mass is favored by increasing temperature because the adsorption reaction is endothermic. This increment value tends to a plateau while the temperature increases from 313 to 318 K.



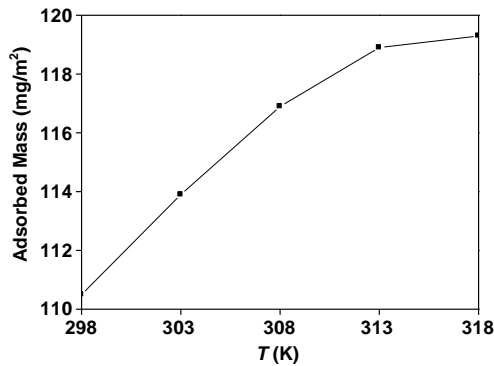


Fig. 7. Effect of temperature of sodium oleate on TiO<sub>2</sub> surface (sodium oleate concentrate 100 mg/m<sup>3</sup>, pH = 5.0)

The standard Gibbs free energy of adsorption value ( $\Delta G$ ), standard enthalpy of adsorption ( $\Delta H$ ), and entropy change ( $\Delta S$ ) were calculated as follow:

$$\Delta G = -RT \ln K \quad (7)$$

$$\ln K = \frac{\Delta S}{R} - \frac{\Delta H}{RT} \quad (8)$$

where  $K$  is the Langmuir equilibrium constant ( $K_L$ ), and  $T$  is the temperature (K).  $\Delta H$  and  $\Delta S$  were calculated from van't Hoff's equation and represented in Table 2 from the slope and intercept of the linear plot of  $\ln K_L$  versus  $1/T$  (Fig. 8).

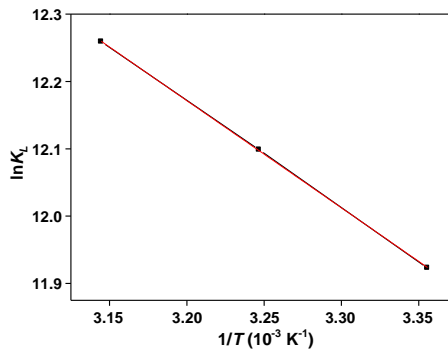


Fig. 8. Van't Hoff's regressions for determination of thermodynamic parameters

As shown in Table 2, the values of  $\Delta G$  confirm the spontaneous nature and feasibility of the adsorption (Auta and Hameed, 2014). Besides, the decrease value of  $\Delta G$  with an increase in temperature suggests the adsorption is more favorable at higher temperature. Researchers have reported that the  $\Delta H$  of physisorption is smaller than 40

kJ/mol (Yao et al., 2010). The value of  $\Delta H$  is 13.23 kJ/mol, indicating sodium oleate adsorption onto TiO<sub>2</sub> coated sensor surface is a physisorption process and the adsorption reaction is endothermic. Meanwhile, the  $\Delta S$  illustrates the randomness of solid-solution interface increased during the sodium oleate onto the active sites of TiO<sub>2</sub> coated sensor surface.

Table 2. Thermodynamics parameters for the adsorption mass of sodium oleate on TiO<sub>2</sub> surface

Temperature (K)	1/T	lnK <sub>L</sub>	$\Delta G$ (kJ/mol)	$\Delta H$ (kJ/mol)	$\Delta S$ (J/(mol·K))
298	0.00336	11.92	-29.53		
308	0.00325	12.10	-30.97	13.23	143.47
318	0.00315	12.26	-32.40		

## Conclusions

Substantial adsorption of sodium oleate solution on TiO<sub>2</sub> coated sensor surface was attributing to electrostatic adsorption with QCM-D analysis. The Langmuir model is suitable to explain the adsorption process, instead of the Freundlich model. The saturation adsorption mass is 111.47 mg/m<sup>2</sup>. The adsorption mass does not change when sodium oleate concentration is greater than CMC. The thermodynamic analysis showed that adsorption is physical, spontaneous and endothermic. The QCM-D technique is a valuable contribution to characterize the adsorption phenomena such as surfactant on solid surface.

## Acknowledgements

This research was subsidized by the Basic Research of Large-scale Quality Improvement and Utilization of Low-quality Coal of "973" Project (Grant No. 2012CB214905).

## References

- AZEVEDO D., ELICH J., MILLER, J.D., 1999, *The effect of pH on pulping and flotation of mixed office wastepaper*, Journal of Pulp and Paper Science, 25(9), 317- 320.
- ALAGHA L., WANG S., YAN L., XU Z., MASLIYAH J., 2013, *Probing adsorption of polyacrylamide-based polymers on anisotropic basal planes of kaolinite using quartz crystal microbalance*, Langmuir, 12, 3989–3998.
- AUTA M., HAMEED B.H., 2014, *Chitosan–clay composite as highly effective and low cost adsorbent for batch and fixed-bed adsorption of methylene blue*, Chem. Eng. J., 237, 350–361.
- BEREKET G., YURT A., 2002, *Inhibition of the corrosion of low carbon steel in acidic solution by selected quaternary ammonium compounds*, Anti-corrosion Methods Mater, 3, 210–220.
- BUTTRY D.A., WARD M.D., 1992, *Measurement of interfacial processes at electrode surfaces with the electrochemical quartz crystal microbalance*, Chem. Rev., 92, 1355–1379.
- CHANTURIA V.A., KONDRAT'EV S.A., 2014, *Mechanisms of nonsulfide mineral flotation with oleinic acid*, J. Min. Sci., 1, 163–170.

- CUI L.M., HU L.H., GUO X.Y., ZHANG Y.K., WANG Y.G., WEI Q., DU B., 2014, *Kinetic, isotherm and thermodynamic investigations of Cu<sup>2+</sup> adsorption onto magnesium hydroxyapatite/ferroferric oxide nano-composites with easy magnetic separation assistance*, J. Mol. Liq., 198, 157–163.
- DENG M.J., XU Z.H., LIU Q.X., 2014, *Impact of gypsum supersaturated process water on the interactions between silica and zinc sulphide minerals*. Miner. Eng., 55, 172–180.
- EBARA Y., OKAHATA Y., 1994, *A kinetic study of concanavalin a binding to glycolipid monolayers by using a quartz-crystal microbalance*, J. Am. Chem. Soc., 116, 11209–11212.
- FAN G.X., LIU J.T., CAO Y.J., HUO T., 2014, *Optimization of fine ilmenite flotation performance in a cyclonic-static micro-bubble flotation column*, Physicochem. Probl. Miner. Process., 2, 823–834.
- FAN X.F., WATERS K.E., ROWSON N.A., PARKER D.J., 2009, *Modification of ilmenite surface chemistry for enhancing surfactants adsorption and bubble attachment*, J. Colloid Interf. Sci., 329, 167–172.
- FAN X., ROWSON N.A., 2000, *The effect of Pb(NO<sub>3</sub>)<sub>2</sub> of ilmenite on ilmenite flotation*, Miner. Eng., 2, 205–215.
- FAN X., ROWSON N.A., 2002, *Surface modification and column flotation of a massive ilmenite ore*, Can. Metall. Quart., 2, 133–142.
- FLEMING B.D., BIGGS S., WANLESS E.J., 2001, *Slow organization of cationic surfactant adsorbed to silica from solutions far below the CMC*, J. Phys. Chem. B., 39, 9537–9540.
- FU J.W., CHEN Z.H., WANG M.H., LIU S.J., ZHANG J.H., ZHANG J.N., HAN R.P., XU Q., 2015, *Adsorption of methylene blue by a high-efficiency adsorbent (polydopamine microspheres): Kinetics, isotherm, thermodynamics and mechanism analysis*, Chem. Eng. J., 259, 53–61.
- GUERRA D.J.L., MELLO I., FREITAS L.R., RESENDE R., SILVA R.A.R., 2014, *Equilibrium, thermodynamic, and kinetic of Cr(VI) adsorption using a modified and unmodified bentonite clay*, Int. J. Mining Sci. Technol., 24, 525–535.
- HACIFAZLIOGLU H., SUTCU H., 2007, *Optimization of some parameters in column flotation and a comparison of conventional cell and column cell in terms of flotation performance*, J. Chin. Inst. Chem. Eng., 38, 287–293.
- IRWIN E.F., HO J.E., KANE S.R., HEALY K.E., 2005, *Analysis of interpenetrating polymer networks via quartz crystal microbalance with dissipation monitoring*, Langmuir, 21, 5529–5536.
- KANAZAWA K.K., GORDON J.G., 1985, *The oscillation frequency of a quartz resonator in contact with a liquid*, Anal. Chim. Acta., 175, 99–105.
- KIM H.J., KWAK S., KIM Y.S., SEO B.I., KIM E.R., LEE H., 1998, *Adsorption kinetics of alkanethiols studied by quartz crystal microbalance*, Thin Solid Films, 327–329, 191–194.
- KOU J., TAO D., XU G., 2010, *Fatty acid collectors for phosphate flotation and their adsorption behavior using QCM-D*, Int. J. Miner. Process., 95, 1–9.
- LI C., LIANG B., GUO L.H., 2006, *Effect of mechanical activation on the dissolution of Panzhihua ilmenite*, Miner. Eng., 19, 1430–1438.
- LILJA M., BUTT U, SHEN Z.J., BJOORN D., 2013, *Nucleation and growth of hydroxyapatite on arc-deposited TiO<sub>2</sub> surfaces studied by quartz crystal microbalance with dissipation*, Appl. Surf. Sci., 284, 1–6.
- MARX K.A., 2003, *Quartz crystal microbalance: a useful tool for studying thin polymer films and complex biomolecular systems at the solution-surface interface*, Biomacromolecules, 4, 1099–1120.
- NEZU T., MASUYAMA T., SASAKI K., SAITOH S., TAIRa M., ARAKI Y., 2008, *Effect of pH and addition of salt on the adsorption behavior of lysozyme on gold, silica, and titania surfaces observed by quartz crystal microbalance with dissipation monitoring*, Dent. Mater. J., 4, 573–580.

- OMIDVAR H., MIRZAEI F.K., RAHIMI M.H., Z. SADEGHIAN, 2012, *A method for coating carbon nanotubes with titanium*, *New Carbon Mater.*, 6, 401–408.
- PADILLA-ORTEGA E., LEYVA-RAMOS R., MENDOZA-BARRON J., 2014, *Role of electrostatic interactions in the adsorption of cadmium (II) from aqueous solution onto vermiculite*, *Appl. Clay Sci.*, 88–89, 10–17.
- PARKER M., STEC B., 2012, *An alternative approach to plating of titanium and Ti alloys using carbon foam substrate*, *Metal Finish.*, 3, 19–22.
- RYU D.Y., FREE M.L., 2003, *The importance of temperature and viscosity effects for surfactant adsorption measurements made using the electrochemical quartz crystal microbalance*, *J. Colloid Interf. Sci.*, 264, 402–406.
- SAKAI K., SMITH E.G., WEBBER G.B., SCHATZ C., WANLESS E.J., BUTUN V., ARMES S.P., BIGGS S., 2006, *pH-responsive diblock copolymer micelles at the silica/aqueous solution interface: adsorption kinetics and equilibrium studies*, *J. Phys. Chem.*, 110, 14744–14753.
- SANTANA R., RIBEIRO J., SANTOS M., REIS A., ATAÍDE C., BARROZO M.A., 2012, *Flotation of fine apatitic ore using microbubbles*, *Sep. Purif. Technol.*, 98, 402–409.
- SAUERBREY G., 1959, *Verwendung von schwingquarzen zur wägung dünner schichten und zur mikrowägung*, *Zeitschrift für Physik*, 2, 206–222.
- SCHUMACHER R., BORGES G., KANAZAWA K.K., 1985, *The quartz microbalance: a sensitive tool to probe surface reconstructions on gold electrodes in liquid*, *Surf. Sci. Lett.*, 1, 621–626.
- SIMBECK T., THOMAIER S., STOCK C., 2011, *Measurement of adsorption kinetics of benzotriazole on copper surfaces via impedance scanning quartz crystal microbalance studies*, *Electrochem. Commun.*, 8, 803–805.
- SOMASUNDARAN P., HUANG L., 2000, *Adsorption/aggregation of surfactants and their mixtures at solid liquid interfaces*, *Adv. Colloid Interface*, 88, 179–208.
- SONG W.L., ZHU Z., MAO Y.N., ZHANG S.S., 2014, *A sensitive quartz crystal microbalance assay of adenosine triphosphate via DNA zyme-activated and aptamer-based target-triggering circular amplification*, *Biosens. Bioelectron.*, 53, 288–294.
- STRYDOM S. J., OTTO D. P., STIEGER N., AUCAMP M. E., LIEBENBERG W., VILLIERS M. M. DE, 2014, *Self-assembled macromolecular nanocoatings to stabilize and control drug release from nanoparticles*, *Powder Technol.*, 256, 470–476.
- VITTORIAS E., KAPPL M., BUTT H., JOHANNSMANN D., 2010, *Studying mechanical microcontacts of fine particles with the quartz crystal microbalance*, *Powder Technol.*, 203, 489–502.
- YAKOVLEVA A. A., CHYONG S. N., 2013, *Kinetic features of the adsorption of sodium oleate on talc*, *Russ. J. Physical Chemistry A.*, 11, 1916–1920.
- YANG Z.P., SI S.H., ZHANG C.J., 2007, *Quartz crystal microbalance studies on bilirubin adsorption on self-assembled phospholipid bilayers*, *J. Colloid Interf. Sci.*, 305, 1–6.
- YAO Y.J., XU F.F., CHEN M., XU Z.X., ZHU Z.W., 201, *Adsorption behavior of methyleneblue on carbon nanotubes*, *Bioresour. Technol.*, 101, 3040–3046.